Two Topics on Plane Tiling

Hiroshi Fukuda[1], Toshiaki Betumiya[2], Shizuka Nishiyama[1], and Gisaku Nakamura[1]

1 School of Administration and Informatics, University of Shizuoka,
52-1 Yada, Shizuoka-shi, Shizuoka 422, Japan
2 ATELIER DAIDALOS,
201, Yoyogi Pearl Heights, 1-9-5, Yoyogi, Shibuya-ku, Tokyo 151, Japan

Abstract

The paper consists of two topics on plane tiling, i.e., tilings with glide-reflection (**pg** tiling) of polyominoes and a solid model for Penrose tiling, that were separately presented at the conference. The former investigates some mathematical characters on **pg** tiling and obtains all polyominoes, from domino (2-omino) to 11-omino, having the **pg** tiling by exhaustive computer search. It is interesting to note that some polyominoes have several different types of **pg** tiling.

The latter investigates the solid model obtained by recursive substitutions of star rhombic dodecahedra with the size of τ^{-3}, where $\tau(= 1.618034)$ is the golden ratio, and finds that Penrose tiling is obtained by a single parallelepipedon, the acute rhombohedra usually denoted by A_6. The result may require some modifications of the theory previously established, in which two kinds of parallelepipeda, the acute and obtuse rhombohedra usually denoted by A_6 and O_6, must be provided.

Keywords: Penrose tiling, Plane tiling, Polyomino, Solid model, Star rhombic dodecahedra

1 pg tiling of polyomino

Escher patterns [1], two-dimensional repeating patterns of a single motif without gaps, or two-dimensional tiling of a single motif, have been studied by many physicists and mathematicians. For example, Husimi and Nakamura proposed a simple method to produce such patterns [2], and Nakamura [3] tabulated motifs which generate Escher patterns having rotational axes. In this work, we use polyominoes [4] or n-ominoes, which are the union of n square cells as a motif of Escher patterns, and consider only **pg** patterns among seventeen two-dimensional patterns [5]. We present all possible **pg** patterns generated by a given n-omino by using an algorithm suitable for computer with $n \leq 11$. We also develop a computer graphics system to generate patterns of larger polyomino.

1.1 Algorithm

A **pg** pattern has glide-reflection axes, that is, the pattern is invariant under operation of reflection and simultaneous translation along the axes. The axes are all parallel and located at equal intervals. We denote the interval of glide-reflection axes by x and length of translation accompanied by the glide-reflection operation by p. In order to tile n-ominoes

on a plane without gaps, these quantities have to satisfy

$$2px = n. \tag{1}$$

Since all boundaries of n-omino are parallel or perpendicular to each other, direction of glide-reflections have to be either parallel (case I) or 45 degrees (case II) to the boundaries of n-omino. Considering the arrangement of cells of the n-omino in the overall pattern, x and p are further restricted to

$$p = \frac{u}{2},\ x = \frac{v}{2},\ u, v = 1, 2, 3, \ldots \tag{2}$$

for case I, and

$$p = \frac{\sqrt{2}u}{2},\ x = \frac{\sqrt{2}v}{2},\ u, v = 1, 2, 3, \ldots \tag{3}$$

for case II.

The glide-reflection axes have to be on vertices of the cell or on the centers of the edges of the cell (4). However, in case I, if u is even and part of the boundaries of the n-ominoes align on the lines perpendicular to the direction of glide-reflection ("cut"), glide-reflection axes can locate any position.

According to the above consideration, we can search all possibilities, which are finite, by a computer and we can obtain all **pg** Escher patterns generated by a given polyomino. The constituent polyominoes must be simply connected. The number of these n-ominoes are 5, 12, 35, 107, 363, 1248, 4460 and 16094 for $n = 4$, 5, 6, 7, 8, 9, 10 and 11, respectively.

Some of the polyominoes are themselves symmetric. Since a polyomino consists of square cells, its symmetries are, in the usual notation of point symmetric groups, either C_1, C_2, C_s, C_{2v} or C_{4v}. On the other hand, the **pg** group has a subgroup of higher symmetric two-dimensional groups, i.e., **pm**, **cm**, **pgg**, **pmg**, **pmm**, **cmm**, **p4g** and **p4m** [5]. Therefore some patterns generated by the algorithm in Section 1 may have these higher symmetries.

In Table 1, we summarize the conditions in which the symmetry of the two-dimensional patterns generated by the algorithm increases with respect to the point symmetry of polyominoes.

Table 1. Symmetry of generated patterns with respect to symmetry of polyominoes

	C_1	C_2	C_4	C_s			C_{2v}		C_{4v}
				$\parallel$	$\perp$	$\angle$	$\parallel$	$\angle$	
pg	$*$	$*$	$*$	$*$		$*$		$*$	
pm				$q = 0$					
cm				$q = x$					
pgg		$q = x$	$q = x$					$q = x$	
pmg		$q = 0$	$q = 0$		$*$		$*$	$q = 0$	$*$
pmm							$q = 0$		$q = 0, p \neq 2x$
cmm							$q = x$		$q = x, p \neq x$
p4g			$p = q = x$						
p4m									$q = x, p = x$ or $q = 0, p = 2x$

The symbols $\parallel$, $\perp$, and $\angle$ imply that the angle between mirror axes of polyominoes and glide-reflection axes of the generated pattern are 0, 90 and 45 degrees, respectively, and $q/2$ is the minimum distance between the center of symmetry of the polyomino and glide-reflection axes. If any conditions tabulated in the row do not hold, the patterns indicated by "$*$" are generated. The above-mentioned algorithm together with Table 1 enables us to generate all Escher patterns of the **pg** family, i.e., the above mentioned nine groups.

1.2 Example for pentominoes

As an example, we exhibit all Escher patterns of the **pg** family generated by pentominoes (5-ominoes) along with symmetry of pentominoes and of patterns. The numbers, such as 5-2, are the n and the label to distinguish n-ominoes and an underscore means that the pattern has a horizontal "cut".

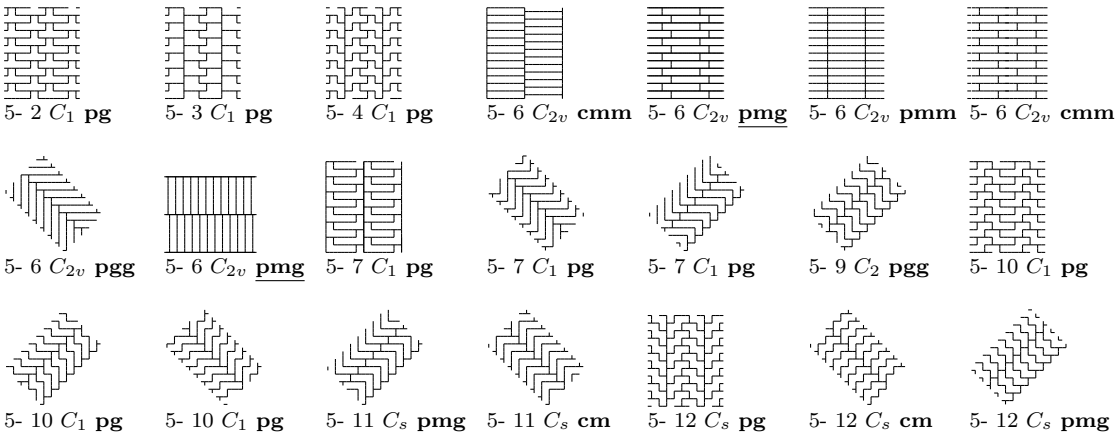

Figure 1: Escher patterns of the **pg** family generated by pentominoes.

It is interesting that the complex polyomino such as 5-12 in Fig. 3 yields the several(three) different **pg** patterns. We have investigated such 'degenerate' patterns among all n-ominoes with $n \leq 11$. In Fig. 2, we show the polyominoes having largest 'degeneracy' of n-omino generating **pg** patterns. Fig. 2(a) is the 10-omino which has the largest degeneracy (=8) and Fig. 2(b) are the polyominoes which have the largest degeneracy (=5) among C_1 polyominoes.

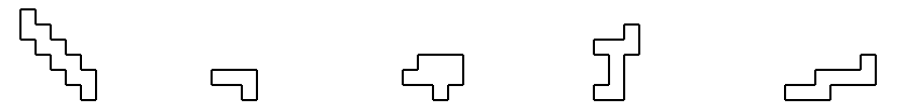

Figure 2: n-ominoes having largest 'degeneracy'.

The five degenerate patterns generated from the polyomino (b.3) in Fig. 2 are shown in Fig. 3. In Table 2, we have tabulated the numbers of polyomino generating **pg** tiling and the numbers of generated independent patterns against both n and symmetry.

Table 2. Number of **pg** tiling

n	1	2	3	4	5	6	7	8	9	10	11
Number of n-ominoes											
C_1	0	0	0	1	5	16	29	129	255	668	462
higher	1	1	2	4	4	14	8	36	35	79	32
total	1	1	2	5	9	30	37	165	290	747	494
Number of patterns											
pg from C_1	0	0	0	5	9	47	46	243	360	1019	716
pg	0	0	1	2	1	8	1	16	6	15	1
higher	3	6	8	15	11	42	17	79	64	132	53
total	3	6	9	22	21	97	64	338	430	1166	770

In the rows labeled "C_1" and "higher" the number of n-ominoes of C_1 symmetry and higher symmetry are tabulated, respectively. In the rows labeled "**pg** from C_1" and "higher" the number of **pg** patterns generated by C_1 n-ominoes and the number of higher symmetric patterns than **pg** are tabulated, respectively. The row labeled simply **pg** shows the number of **pg** patterns generated by polyominoes having higher point symmetry than C_1. The patterns which can be superposed by rotation and reflection are considered to be same.

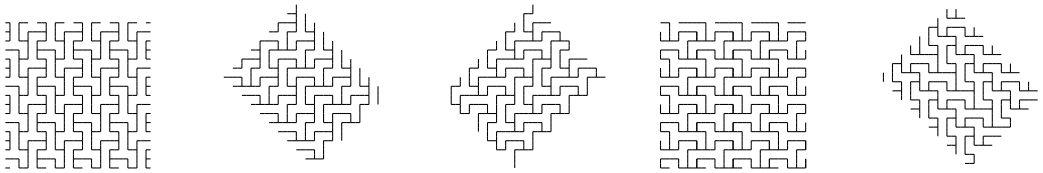

Figure 3: Five 'degenerate' patterns (8-omino).

1.3 Graphics system

We have developed a computer graphics system to generate more complex **pg** patterns on the graphical operating system, MS-Windows 3.1$^{\text{TM}}$. The shape of the elements of the picture on the graphics display supported by MS-Windows is square, or omino. Thus, all pictures on graphics display are polyomino but they are composed of a large number of ominoes.

Our graphics system modifies the n-omino given in previous sections. It decomposes ominoes in n-omino to $k \times k$ smaller ominoes, regards the n-omino as k^2n-omino, and then adds the ominoes around the boundary or deletes the ominoes on the boundary. When an omino is added, some omino on the boundary is deleted and this correspondence is one-to-one. When an omino is deleted, some omino is added on the boundary but this correspondence is one-to-g with $1 \leq g \leq 3$.

After the above modification, the point symmetry of the original n-omino is lost generally and modified patterns become purely **pg**. For the patterns having space symmetry **pgg**, **pmm**, **cmm** and **p4m** we can change the direction of glide-reflection axes, and for the patterns having "cut" as discussed in Section 1, we can change the location of glide-reflection axes. Our system accounts for these aspects of freedom of a given pattern of n-omino and we can do all these operations on the system graphically. Figure 4 shows an example of modified **pg** pattern by our system, which consists of $4^2 \times 8$ ominoes.

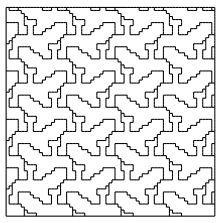

Figure 4: **pg** pattern generated by our graphics system.

2 A solid model for Penrose tiling

A solid model for Penrose tiling [6] is proposed, by using star rhombic dodecahedra, each vertex of which is recursively substituted by a smaller star rhombic dodecahedron. The proposed model happened to be obtained by one of the authors, Betumiya, in the process of devising a 3-dimensional mathematical puzzle. The model seems to suggest that Penrose tiling has a 5-fold rotational symmetry in the strict sense, and its structure may not be an intermediate state between crystalline and amorphous states [7], [8].

Figure 5(a) is a famous photograph of the electron diffraction pattern of a quasi crystal of Fl-Fe-Cu, from which a 5-fold rotational symmetry is observed [9]. Figure 5(b) is a crude sketch of the proposed solid model, which is explained later. Comparing Fig. 5(a) with Fig. 5(b), a remarkable resemblance can be observed.

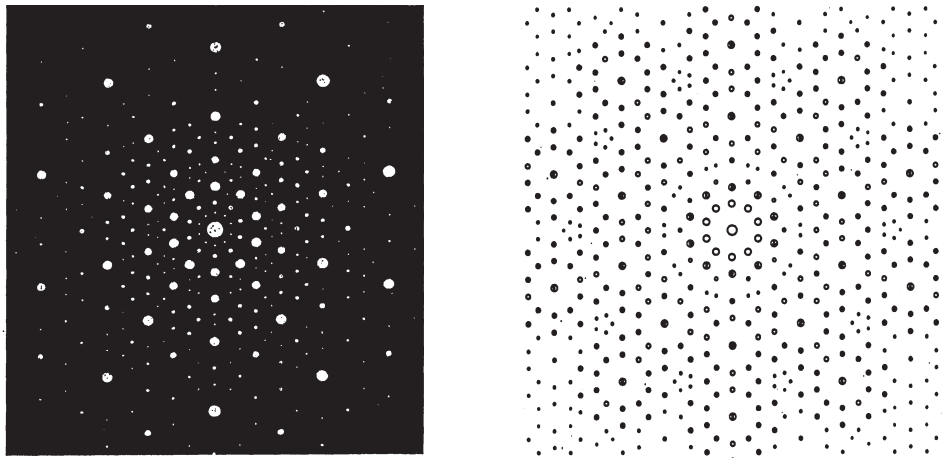

(a) (b)

Figure 5: Electron diffraction pattern and the proposed solid model.

The left side of Fig. 6 is an icosahedron and the right side is a star rhombic dodecahedron which is obtained from the icosahedron by attaching 20 paralellepipeda of A_6 on the 20 regular triangle facets, respectively, in the usual way. It is assumed that the length of each edge of the star rhombic dodecahedron is 1.

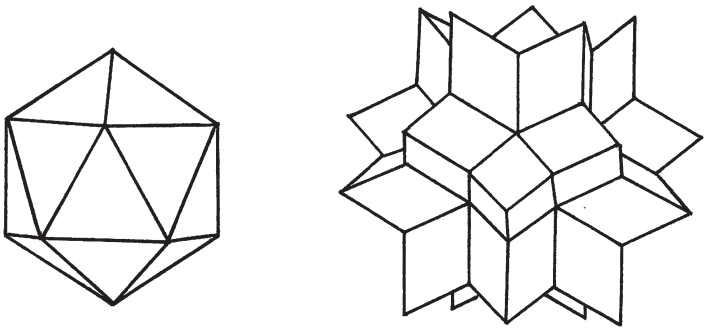

Figure 6: An icosahedron and a star rhombic dodecahedron.

Figure 7(a) is a precise figure of the same star rhombic dodecahedron observed in a normal direction, where the normal direction means the figure has a 5-fold rotational symmetry.

Provide a 62 star rhombic dodecahedra with the length of edge τ^{-3}, where $\tau(= 1.618034)$ is the golden ratio, and substitute them for the vertices of the original star rhombic dodecahedron, respectively, as follows:

Coincide the center of each smaller star rhombic dodecahedron with one of the vertices of the original star rhombic dodecahedron, and then, rotate it as the figure has a 5-fold rotational symmetry in the direction of the center of the original one. The solid model obtained is like a cactus of star rhombic dodecahedra with two different sizes. The solid model is called a 2-fold cactus. Figure 7(b) is the precise figure of the 2-fold cactus looked at in a normal direction, where the duplicated lines are the original edges of Fig. 7(b). Then, Fig. 5(b) shown previously is obtained from Fig. 7(b); if all the edges are deleted, a light circle is used for a single vertex, and a dark circle is used for overlapped vertices.

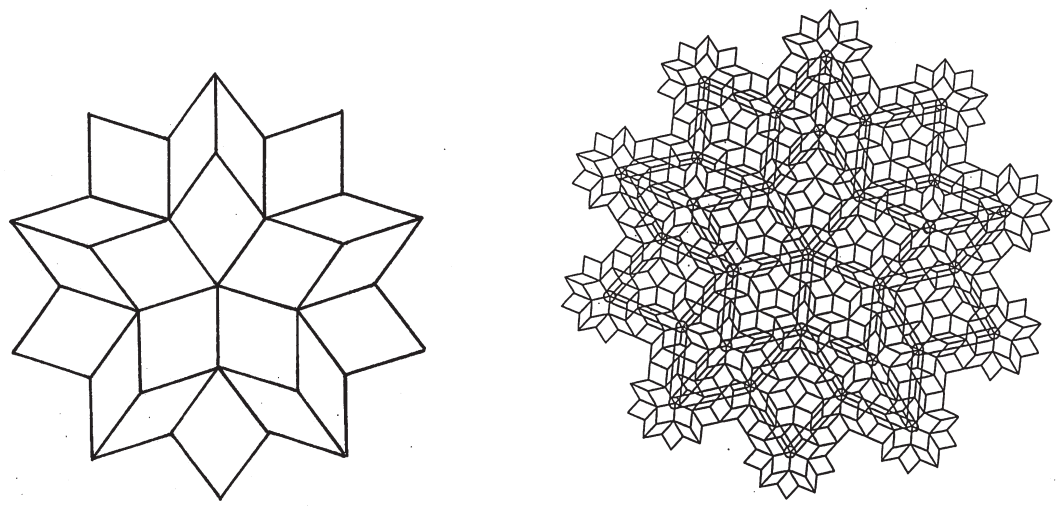

(a) (b)

Figure 7: Star rhombic dodecahedron and 2-fold cactus.

The above substitution is made recursively. Provide a 62^2 star rhombic dodecahedra with the length of edge $\tau^{-6}(= 0.0557)$, and substitute them for the vertices of the 2-fold cactus, respectively. Then, the 3-fold cactus is obtained. In the same way, the k-fold cactus is obtained by substituting 62^{k-1} star rhombic dodecahedra with the length of edge $\tau^{-3(k-1)}$ for the vertices of $(k-1)$-fold cactus, respectively. A Penrose pattern is obtained as the figure of the k-fold cactus looked in a normal direction, where k increases infinitely. It is noted that the paralellepipeda of O_6 occur automatically in this model as the vacancies.

There is an interesting experiment for visualizing the proposed solid model. Provide five pieces of isosceles triangle mirrors shown in the left side of Fig. 8, and assemble them into a pentagonal cone the inside of which is mirror faces, shown in the right side of Fig. 8.

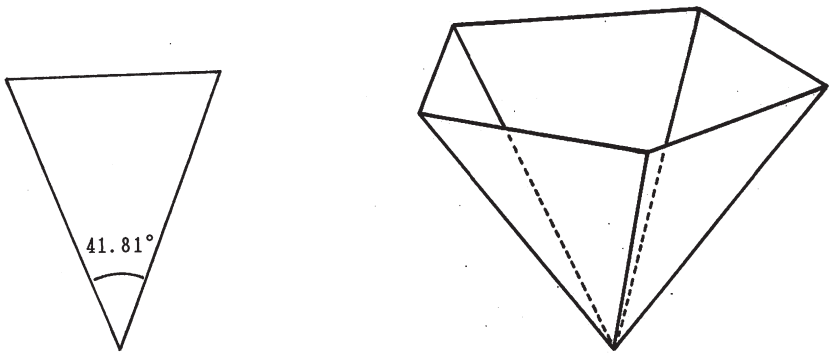

Figure 8: Isosceles triangle and pentagonal cone.

Next, provide five sheets of rhombuses as shown in the left side of Fig. 9, and put them on the mirror faces of the pentagonal cone as is shown in the right side of Fig. 9. Peeping on the inside of the cone, a desired star rhombic dodecahedron appears. It is noted that the shape of the rhombus in the left side of Fig. 9 completely coincides with that of a facet of a triacontahedron. If the number of the rhombuses is increased in an ingenious way, the proposed solid model appears. It is noted that there are several interesting properties, which were stated in the aural presentation, as well as an exhibition of the proposed solid model.

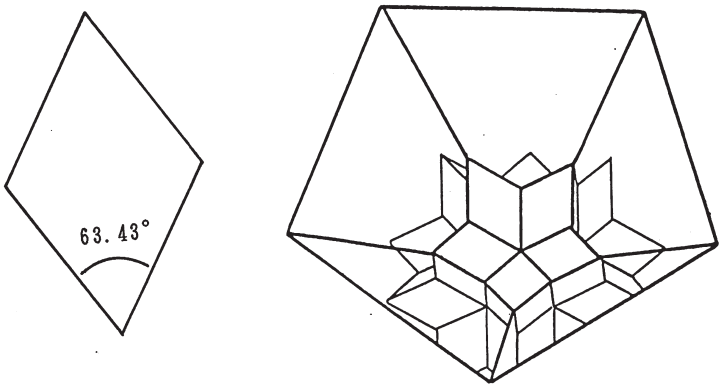

Figure 9: Rhombus and the mirror faces.

References

[1] C. H. Macgillavry, *Symmetry aspects of M. C. Escher's periodic drawing*, The International Union of Crystallography, 1976.

[2] K. Husimi, and G. Nakamura, *Escher gahou no himitu wo toku* (in Japanese), Kagaku Asahi, May, **79**, 1979.

[3] G. Nakamura, *Escher no e kara kesshou kouzou he* (in Japanese), Kaimeisha, Tokyo, 1983.

[4] D. A. Klarner, *The Mathematical Gardner*, Prindle, Weber & Schmidt, Boston, 1981.

[5] H. S. M. Coxeter, and W. O. J. Moser, *Generators and Relations for Discrete Groups*, Springer-Verlag, New York, 1965.

[6] R. Penrose, *Math. Intell.*, **2**, 32–37, 1979.

[7] P. Kramer, and R. Neri, *Acta Cryst.*, **A40**, 580–587, 1984.

[8] T. Ogawa, *Scientific American* (Japanese Edition), **16**, 10–23, 1986.

[9] Search & Discovery, *Physics Today*, **38**, 17–19, 1985.